2890 *Macromolecules* **2010**, *43*, 2890–2896
DOI: 10.1021/ma902865e

Macromolecules
ARTICLE

Continuous Cooling Curves Diagrams of Propene/Ethylene Random Copolymers. The Role of Ethylene Counits in Mesophase Development

Dario Cavallo,[†] Fiorenza Azzurri,[†] Roberto Floris,[†] Giovanni C. Alfonso,*[,†] Luigi Balzano,[‡] and Gerrit W. Peters[‡]

[†]*Università di Genova, Dipartimento di Chimica e Chimica Industriale, via Dodecaneso, 31-16146 Genova, Italy, and* [‡]*Department of Mechanical Engineering, Eindhoven University of Technology P.O. Box 513, 5600 MB Eindhoven, The Netherlands*

Received December 30, 2009; Revised Manuscript Received February 5, 2010

ABSTRACT: A simple method to investigate polymer crystallization during fast cooling, based on *in situ* temperature acquisition and ex-situ structural characterization, is proposed. The approach enables one to obtain the continuous cooling curve (CCC) diagrams, widely used in metallurgy but seldom adopted for semicrystalline polymers. This method is here exploited to gain new insights on polymorphic behavior of quenched polypropylene and its copolymers with ethylene. Experimental CCC diagrams, covering a wide range of crystallization temperatures in the domains of monoclinic structure and mesophase, are obtained for the first time. The role of counits in affecting the development of the mesophase upon fast cooling is assessed: the critical cooling rate above which a predominant fraction of mesomorphic form is generated significantly decreases with increasing comonomer concentration. This is due to the remarkable hindrance of ethylene counits on the crystallization kinetics of the α-form, which indirectly favors the development of the less affected mesophase. We expect that this concept can be extended to any kind of defects that disturbs the structuring of the monoclinic phase.

Introduction

In actual processing conditions polymers solidify at cooling rates which span over a wide range, from a few to hundreds of degrees celsius per second, far beyond those accessible by common laboratory instrumentation. Fast cooling results in the development of structural order at extreme undercooling and, for some polymers, this leads to formation of metastable states.[1−3] For its industrial relevance, as well as for its intriguing scientific aspects, isotactic polypropylene represents a paradigmatic example. In fact, a metastable phase characterized by a degree of order intermediate between that of the amorphous and the monoclinic structure, usually referred to as mesophase, is often found in quenched samples.[4−7] Its metastable nature was thoroughly investigated over the last decades,[8−10] and its transition to the thermodynamically stable α-phase has been explored in detail.[11−14]

Piccarolo et al.[15−19] extensively studied polypropylene crystallization in a wide range of cooling rates, from those attainable with DSC, up to ca.10^{-1} °C/s, to the very high ones encountered in processing, up to 10^{3} °C/s. On increasing the cooling rate a gradual decrease in density is initially observed, followed by a further drop at about 100 K/s. The revealed change in density reflects the continuous variation of the relative amount of the two polymorphs, from the pure monoclinic α-phase to the mesophase.[20]

Online crystallization studies of i-PP during fast cooling were performed by Ding and Spruiell using a modified microscopy hot stage.[21] They measured the temperature directly inside a thin polymer film with the aid of a microthermocouple, and detected a temperature plateau in the cooling curve. This plateau is the result of the balance between the rate of heat release due to the first order phase transition and the heat flux to the cooling medium; as a consequence, the crystallization process mainly occurs in pseudoisothermal condition. This evidence was later exploited by Phillips et al. to measure the spherulitic growth rate at previously unattained undercoolings.[22,23]

A similar approach was adopted by Titomanlio et al.,[24−26] but the maximum cooling rate achieved with their system was not sufficient to enter the region of mesophase development. This limitation was overcome by the development of thin film nanocalorimetry, which allows studies of polymer crystallization under cooling rates of the order of several thousand °C/s.[27] Schick et al.[28,29] successfully applied this technique to investigate i-PP crystallization at high cooling rates and confirmed that, below ca. 90 °C/s, crystallization occurs in the α-form. However, on increasing the cooling rate to above 150 °C/s, a second exothermic signal, which must be assigned to mesophase structuring, is detected in the temperature range from 40 to 20 °C. By further increasing the cooling rate, the α-form is fully inhibited and only the mesomorphic phase develops at around room temperature. Eventually, at cooling rates exceeding 1000 °C/s, also the formation of the mesophase is prevented and i-PP solidifies in a fully amorphous state. Through a series of isothermal crystallization experiments at extreme undercoolings, down to 5 °C, Schick et al. demonstrated that two bell-shaped curves, which intersect at ca. 45 °C, are required to describe the temperature dependence of the crystallization rate constant. As it was already predicted from kinetic models based on off-line structure content determination,[20,30] this variation in kinetic behavior is clearly linked to the kinetically controlled development of the mesophase.

A convenient way of tackling the issue of materials' polymorphic behavior and, in a wider perspective, of their crystallization under fast cooling, is through the continuous cooling curves (CCC) diagrams. CCC diagrams, and their analogous

*To whom correspondence should be addressed. E-mail: alfonso@chimica.unige.it.

 Published on Web 02/12/2010

isothermal counterparts, i.e., the time, temperature, transformation (TTT) diagrams, are widely used in metallurgy to correlate the specific transformations occurring in the material (e.g., austenite to pearlite in steel) with the imposed thermal history.[31,32] Despite its potential, this approach has seldom been adopted for semicrystalline polymers, even though its importance for the interpretation of polymer structuring in complex processing conditions has been recognized.[33−35]

Iso-transformation curves, obtained from DSC experiments in relatively slow cooling conditions, were reported for PEEK.[36,37] However, to our knowledge, only one paper dealing with CCC and the polymorphic behavior of polypropylene has been published so far.[38] In that work, focused on melt spinning, a wide collection of experimental data was presented and used to relate the structure of the solidified polymer to the processing conditions. The most important result was the enhancement of the α-phase crystallization rate due to the applied spinline stress, which prevents mesophase formation even under severe quenching conditions. This was clearly pointed out by means of the CCC diagrams, which provide a powerful tool to investigate the effect of any variable affecting crystallization rate.

We believe that the potential of CCC diagrams could further be exploited through a new approach which combines in situ temperature measurements during fast cooling with ex-situ WAXD structural characterization. The proposed method is here applied to study the crystallization of isotactic polypropylene containing randomly distributed constitutional defects, i.e. ethylene counits. The detailed studies of Alamo et al.[39−41] and of De Rosa et al.[42−44] demonstrated that the presence of various types of chain defects in isotactic polypropylene affects the crystallization kinetics and the formation of the α- and γ-polymorphs in relation to the level of inclusion of defective units into the respective crystal lattices. However, their comprehensive investigations did not include conditions in which the mesomorphic phase forms. The role of molecular features in the development of this metastable structure still waits for exhaustive experimental evidence.

Hereby, through the CCC diagrams approach, we provide new experimental results which highlight the effect of ethylene counits on polypropylene polymorphism at high cooling rates.

Materials and Methods

Materials. The materials used in this study are a commercial Ziegler−Natta isotactic polypropylene homopolymer and two random copolymers with ethylene, kindly provided by Borealis. As shown in Table 1, these polymers differ only in the ethylene content, while average molar mass and molar mass distribution are identical. Thus, they are good candidates to investigate the effect of small constitutional defects on the development of different types of structural order upon quenching. Consistently with their composition, in standard DSC experiments performed using a cooling rate of 10 °C/min, the copolymers crystallize at progressively lower temperature and to less extent on increasing the comonomer content.[45,46]

Polymer films around 150 μm thick, suitable for the intended characterization of their crystallization behavior at high cooling rates, were obtained first from the supplied pellets by compression molding at 210 °C for 5 min and subsequent quenching in air.

Methods. To monitor the actual specimen temperature during fast cooling, a calibrated Chromel-Alumel μ-thermocouple (50 μm diameter wires) was embedded between two polymer films 20 × 50 mm which were then tightly wrapped in a thin aluminum foil. The positioning of the thermocouple was done by melting one film on a hot stage, placing the temperature sensor on its surface and then superposing the second film. While in the molten state, a slight pressure was imposed on the sample with the help of a microscope cover glass before cooling to room temperature. The polymer sandwich was then cut to the suitable dimensions with a razor blade and wrapped with a single 20 μm thick aluminum foil.

Table 1. Main Features of the Materials under Investigation

C2 content (mol %)[45]	M_w (kg/mol)	M_w/M_n	T_c (°C)	ΔH_c (J/g)
0	310	3.4	112.0	−94.6
3.4	310	3.4	103.0	−81.3
7.3	310	3.4	96.1	−64.8

Measurements were performed according to the following procedure. First, the system was heated to 220 °C in a hot stage and there held for 5 min to erase any memory effect; next, the sample was quenched while recording the instantaneous temperature using a fast acquisition datalogger (HP 34970A, sampling frequency 25 Hz). The cooling fluid was either a large volume of water at different temperatures (in which the sample was dipped) or room temperature air, blown on sample's large surfaces with different flow rates. Typical temperatures of the cooling media were 20, 10, 0, and −10 °C. To obtain the low temperatures, water/ice and water/ice/NaCl mixtures were used as quenching baths. Detailed analysis of the measured cooling curves will be discussed in the next section.

The final structure of the quenched samples was probed by wide angle X-ray diffraction with a Bruker AXS SMART 1 k CCD diffractometer; Cu Kα radiation (wavelength 1.54 Å) and a sample to detector distance of 10 cm were used. To quantitatively determine phase contents, after subtraction of the air scattering, the WAXD patterns were deconvoluted according to a standard procedure[19,30,47] using the software package PeakFit. The actual WAXD pattern is considered to be the superposition of the intensity of the whole set of reflection associated with all types of structural order. Seven Pearson VII type curves were used to describe the α-phase ($2\theta = 14.1°, 16.9°, 18.6°, 21.4°, 22.1°, 25.5°$, and $28.5°$), two broad Pearson VII curves for the mesomorphic phase ($2\theta = 15.1°, 21.3°$) and a broad, asymmetric, Pearson IV ($2\theta \approx 17-18°$) was adopted for the amorphous halo.[47] The value of the Bragg distances of the α-form and of the mesophase was observed not to depend on cooling rate,[14] nor on ethylene content in the copolymer.[43] Contribution of the γ-form to the diffracted intensity were not detected and contemplated in the deconvolution because this polymorph does not develop at the imposed high cooling rates.[48] A good fit, confirmed by a Pearson correlation coefficient, r^2, larger than 0.99, was always achieved. The amount of the different phases was calculated as the ratio between the area of the corresponding peaks to the total area of the pattern. An uncertainty of ±3% on the absolute value of phase contents was estimated, well in agreement with typical errors for this type of deconvolution.[30]

Results and Discussion

Data Analysis and Construction of CCC Diagrams. To analyze the quenching process, an approach similar to that used by Ding and Spruiell[21] is adopted. The basic assumption is that the temperature gradient across the sample is negligible. Detailed heat transfer analysis of analogous experiments has shown that, for the range of sample thickness and cooling rates explored in this work, this is a good approximation.[18,21,49] The evolution of sample's temperature is dictated by the heat exchange with the cooling medium, which is at a constant temperature. When no phase transition takes place, the result is a simple exponential law ("natural" cooling):

$$T(t) = T_\infty + [T(0) - T_\infty] \exp[-Bt] \quad (1)$$

where T_∞, is the temperature of the environment, $T(0)$ is the initial temperature of the molten polymer and B is a characteristic time constant for the cooling process, which

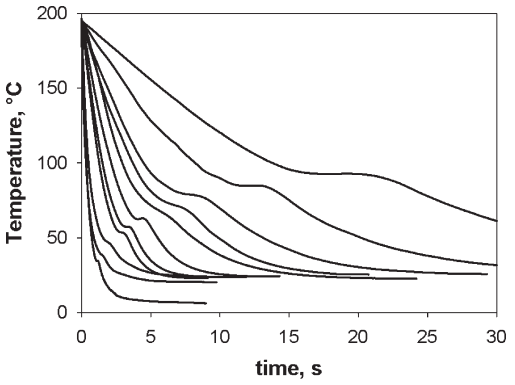

Figure 1. Examples of cooling curves obtained for the copolymer with 3.4 mol % of ethylene counits at different air flow rates or bath temperatures.

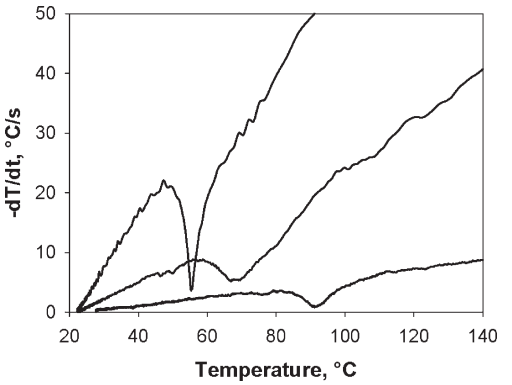

Figure 2. Examples of instantaneous cooling rate as a function of temperature for the copolymer with 3.4 mol % of ethylene counits. For the sake of clarity, only three curves are shown.

depends on the overall heat exchange coefficient (sample geometry, fluidodynamic conditions in the boundary layer, material's properties, ...). The resulting instantaneous cooling rate is linearly dependent on the actual sample's temperature and is given by:

$$\left(\frac{dT}{dt}\right)_{nat.cool} = -B[T(0) - T_\infty]\exp[-Bt] = -B[T(t) - T_\infty] \quad (2)$$

Taking into account the heat released in the crystallization process, the overall experimental cooling rate can be written as

$$\left(\frac{dT}{dt}\right)_{exp} = \left(\frac{dT}{dt}\right)_{nat.cool} + \left(\frac{dT}{dt}\right)_{cryst} = -B[T(t) - T_\infty] + \frac{\Delta H_c^0}{c}\frac{dx}{dt} \quad (3)$$

where ΔH_c° is the latent heat of the phase transition, c is the averaged specific heat of the system, and dx/dt is the crystallization rate. Therefore, when crystals begin to develop, a deviation from linearity in the cooling rate vs temperature plot should be observed.

As an example, a series of typical $T(t)$ curves, recorded during cooling in different media, is shown in Figure 1 for the copolymer with 3.4 mol % of ethylene counits. In this plot, zero time was assigned to the instant at which the temperature was crossing 195 °C during the cooling from a slightly higher temperature (220 °C). This rescaling of the time axis is based on the consideration that 195 °C is a fair estimate of the equilibrium melting temperature of the α-form of i-PP.

A clear manifestation of the effect that the heat released by the crystallizing polymer has on the cooling process is a temperature plateau, which is particularly evident when relatively slow cooling is imposed. This plateau has been previously observed and corresponds to a pseudoisothermal crystallization temperature occurring when the latent heat is released at a rate which is comparable to the heat flux toward the cooling medium.[21−24,35] These conditions are fulfilled only in mild quenching experiments; instead, the temperature plateau is missing at high cooling rates and the phase transition is hard to be detected directly from the $T(t)$ curves. An unambiguous and highly reproducible feature is required to characterize the crystallization process also under very fast cooling regimes. This feature can be obtained by plotting the instantaneous cooling rate as a function of actual specimen temperature, as shown in Figure 2. According to eq 3, a linear relationship between cooling rate and temperature is observed whenever the cooling process is not perturbed by crystallization. In the temperature range in which the phase transition takes place, the cooling rate exhibits a relatively sharp drop and then increases again when the instantaneous latent heat release is overcome by the heat flux toward the medium. The temperature, T_{onset}, at which the curve deviates from linearity corresponds to the crystallization onset, while the minimum coincides with the maximum rate of transformation. This minimum is chosen as the characteristic crystallization temperature, T_c, in analogy with the crystallization peak temperature measured in classical DSC experiments. A suitable parameter to characterize the cooling history is also required. To this aim, Ding and Spruiell adopted the cooling rate function,[21] i.e., the time constant in the exponential decay of temperature, while Piccarolo et al.[18−20] used the measured cooling rate at 70 °C, which is supposed to correspond to the temperature at which PP exhibits the largest crystallization rate-constant. A suitable alternative option, which is not affected by the crystallization itself, is the use of the average cooling rate, defined as the slope of the straight line connecting the origin of the $T(t)$ curve (T = 195 °C, t = 0 s) to the onset of the phase transition.

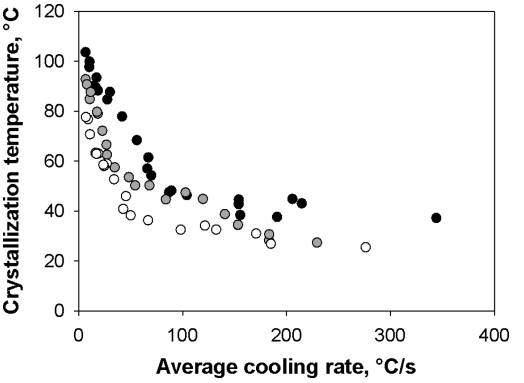

Figure 3. Crystallization temperature as a function of average cooling rate for the P/E random copolymers. Key: (●) i-PP homopolymer; (gray circle) random copolymer, 3.4 mol % of ethylene; (○) random copolymer, 7.3 mol % of ethylene.

Accordingly, the crystallization temperature of polypropylene and propene/ethylene random copolymers in a wide range of cooling conditions, up to above 300 °C/s, are plotted in Figure 3 as a function of the average cooling rate. For each polymer, the crystallization temperature decreases on increasing the cooling rate; moreover, it is also evident that,

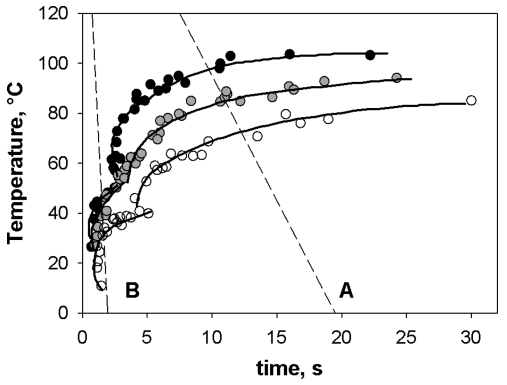

Figure 4. CCT diagrams for P/E random copolymers. Key (●) i-PP homopolymer; (gray circle) random copolymer, 3.4 mol % of ethylene; (○) random copolymer, 7.3 mol % of ethylene. Lines are drawn to guide the eyes. Two representative cooling histories from 195 °C are added as example: (A) constant cooling rate of 10 °C/s; (B) constant cooling rate of 100 °C/s.

under any quenching condition, this temperature is lower the higher the comonomer concentration is. A distinctive feature of the data shown in Figure 3 is the presence of a kink, at around 40−50 °C, which divides the curve into two parts. A very steep decrease of T_c is observed at relatively low cooling rates, while a much weaker dependence is found under more severe quenching.

An alternative and instructing way of looking at these data is offered by the so-called continuous cooling curves (CCC) diagrams, which link temperature and time of crystallization. This powerful approach, which is extensively adopted for metals and metallic alloys, has only seldom been used to describe crystallization in polymeric materials.[33−38]

Figure 4 collects the CCC diagrams of the i-PP homopolymer and of the two copolymers. The plotted data correspond to the time and temperature coordinates at which the cooling rate exhibits its relative minimum. Here, the two crystallization regimes noted in Figure 3 become particularly evident: for each polymer a double "nose" features the temperature−time plots. The part of the curve at higher temperatures corresponds to the development of the α-modification, while the other part can be assigned to the formation of the mesomorphic phase. In terms of crystallization temperature, the crossover from one crystallization regime to the other is located between 50 and 40 °C. This interpretation is corroborated by the isothermal crystallization results obtained by De Santis et al.[29] using ultrafast nanocalorimetry.

With the aid of this diagram, the prevailing structure of the polymer solidified under any cooling history can be inferred. When the cooling curve deeply intersects the upper region of the CCC diagrams (slow cooling, curve A in Figure 4) the polymer crystallizes in the pure α-form. On the contrary, at high cooling rates (curve B), the development of the α-form is bypassed because the intersection occurs only with the nose at low temperatures, thus leading to a mesomorphic phase embedded in an amorphous matrix. At intermediate cooling rates both structures are formed since the short time spent in crossing the α-region leaves enough noncrystalline fraction to further structure when entering the mesomorphic region.

The effect of ethylene counits on the crystallization process under fast cooling conditions clearly results from the CCC diagrams. At a given cooling rate, crystallization in the α-form takes place at progressively lower temperatures and longer times on increasing the comonomer content. This indicates that the presence of randomly distributed constitutional defects strongly depresses the crystallization kinetics of the α-phase also in nonisothermal conditions. Similar conclusions were reached in the detailed work of Alamo et al. on a series of metallocenic propene-ethylene random copolymers.[50] At a given isothermal crystallization temperature, a remarkable increase of crystallization half-time on increasing ethylene content was reported. In addition, a downward shift of the temperature at which the crystallization rate is maximum was also observed. In our CCC diagrams this result is reflected by the shifting of the apex of the α-form nose from ca. 70 °C for the homopolymer to ca. 50 °C for the copolymer with 7.3 mol % of ethylene.

Isothermal crystallization experiments at the very high undercooling required for the development of the mesomorphic structure cannot be performed with commonly available calorimeters and can only be conceived by adopting fast scanning nanocalorimetry.[29] So far, this has forbidden experiments aimed at establishing the role of comonomeric units on mesophase crystallization. The data collected with our simple and inexpensive approach enable us to get some relevant feature on this issue. Compared to the monoclinic form, the development of the mesomorphic phase is affected to a lesser extent by the presence of the comonomer. In facts, the CCC diagrams suggest that, for what concerns the mesophase formation, the apex temperature of the noses is always found in the same narrow temperature range and the corresponding time is increased only slightly by the presence of ethylene units.

These evidence can be explained by considering that constitutional defects can be hosted in the mesomorphic phase with a free energy penalty which is substantially smaller than that for their inclusion into the denser monoclinic structure. Indeed, Alamo et al.[51] have demonstrated that ethylene counits are preferentially excluded from the α-phase lattice.

The tendency of copolymers to develop the mesomorphic structure is easily deduced from the CCC diagrams. The maximum cooling rate at which α-phase crystals can be found in fast cooled samples progressively decreases on increasing the concentration of chain defects. In other words, while under given cooling conditions the homopolymer and the copolymers with small content of ethylene counits crystallize exclusively in the α-form, the copolymers with relatively high concentration of constitutional defects exhibit a predominant mesomorphic order. To prove these statements, the crystalline structure of a number of quenched samples was assessed by means of wide angle X-ray diffraction.

Phase Content Determination by WAXD. Examples of wide angle X-ray diffraction patterns of P/E random copolymers solidified in different conditions are shown in Figure 5. For the homopolymer, as well as for the two investigated copolymers, the transition from α to mesomorphic structure is clearly evident on increasing cooling rate. In addition, the patterns of samples cooled at around 60 °C/s provide unquestionable evidence that the mesophase content increases with the mole fraction of ethylene in the copolymer. In order to assess this trend in quantitative terms, deconvolution of WAXD patterns was performed as earlier described.[19,30,47]

Fractional amounts of α, mesomorphic, and amorphous phases were evaluated for the three polymers submitted to a wide range of cooling rates, from ca. 10 to 300 °C/s. Data pertaining to the copolymer with 3.4 mol % of ethylene are shown in Figure 6; they are representative of the general trend found also for copolymers with bulkier counits and for homopolymers with different degree of stereoregularity.[52] Only a minor increase of the amorphous fraction results in the covered range of cooling rates. Instead, the amount of the

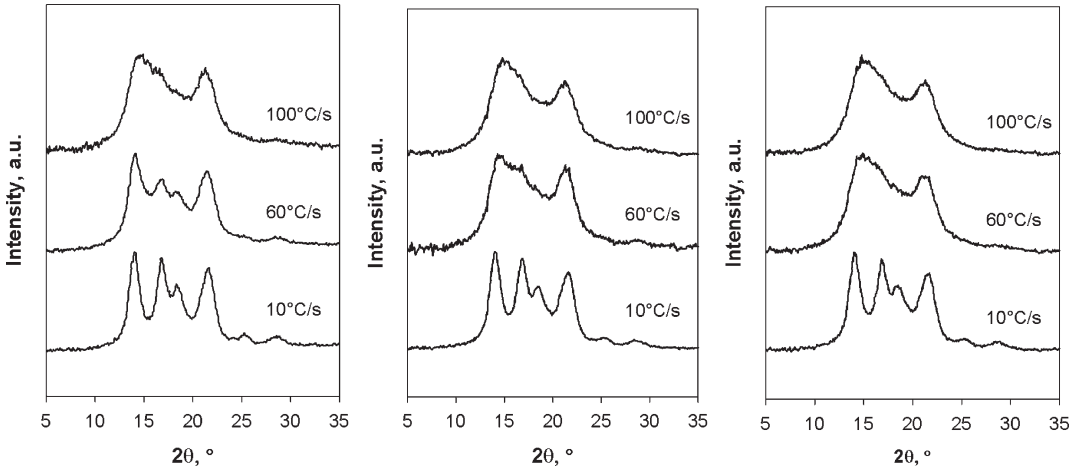

Figure 5. WAXD patterns of C3C2 copolymers quenched at different cooling rate. From left to right: C2 content of 0, 3.4, and 7.3 mol %. Approximate average cooling rate is reported on the plots.

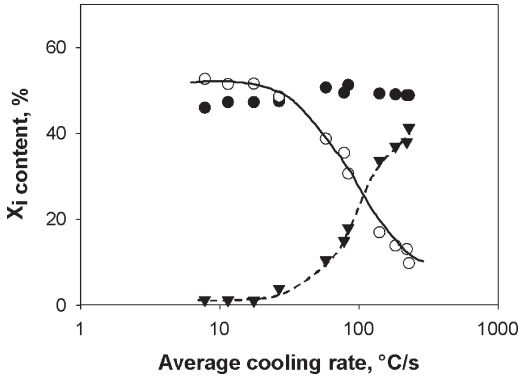

Figure 6. Phase contents from deconvolution of WAXD patterns as a function of the cooling rate for the copolymer with 3.4 mol % of ethylene counits. Lines are inserted to guide the eye. Key: (●) amorphous phase; (○) α-phase; (▼) mesophase.

two competing types of ordered phases undergoes noteworthy changes: at relatively low cooling rates the structure is dominated by the α-phase, while the mesomorphic form prevails in fast cooled samples. The transition between α-phase and mesophase crystallization takes place in a range of cooling rates. The critical value of this variable, which we define as the crossover of the sigmoidal curves describing the experimental data and which represents the transition to a prevailing mesomorphic structure can be extracted. This behavior is already well-known and widely documented in the literature by the extensive work done by Piccarolo et al.[14−20] and Titomanlio et al.[24−30] on i-PP homopolymers. Our results demonstrate that also propene/ethylene random copolymers behave similarly and enable us to assess the role of constitutional defects on the structures which develop at high cooling rates.

The outcome of the deconvolution of WAXD patterns collected at room temperature from samples cooled at different rates is shown in Figure 7a−c. Under similar cooling regimes, a slight decrease of crystallinity can be appreciated on increasing the ethylene content. For all polymers, the number of different imposed cooling conditions was adequate to obtain only crystals of the α-form, at cooling rates lower than ca. 30 °C/s, or predominant mesomorphic order, under the fastest cooling regimes. This enables us to evaluate, with fair accuracy, how the above-defined critical cooling rate changes with the copolymer composition; this

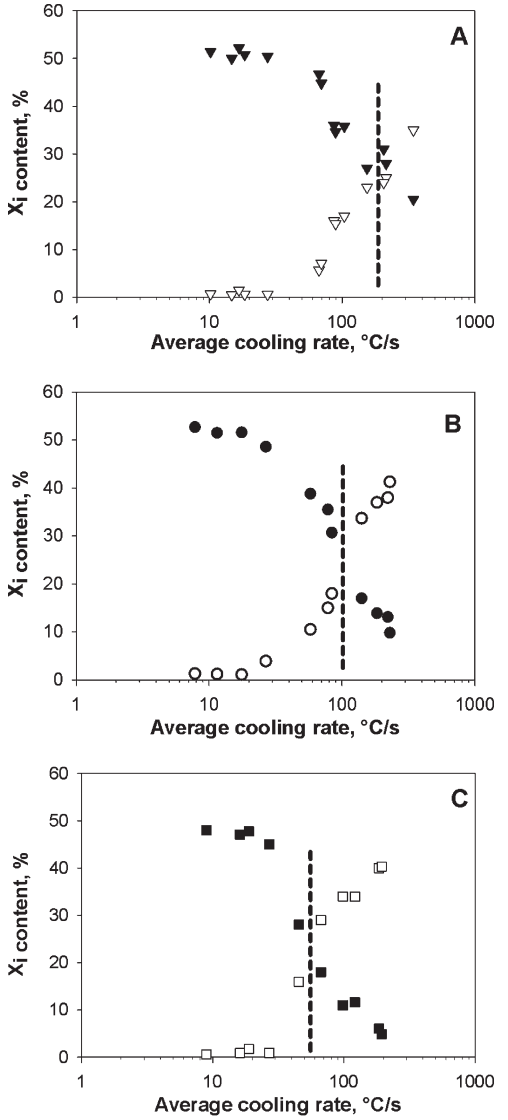

Figure 7. Phase content as a function of average cooling rate for the different P/E random copolymers. Amorphous phase is omitted for the sake of clarity. The critical cooling rate for structural crossover is indicated by a dashed line. Key: (A) i-PP homopolymer; (B) random copolymer with 3.4 mol % of ethylene; (C) random copolymer with 7.3 mol % of ethylene. Filled symbols: α-phase. Open symbols: mesophase.

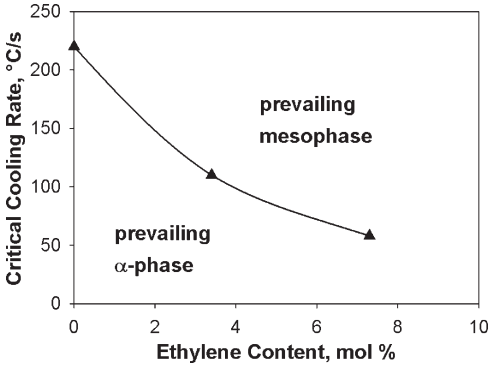

Figure 8. Critical cooling rate for structural crossover versus ethylene content.

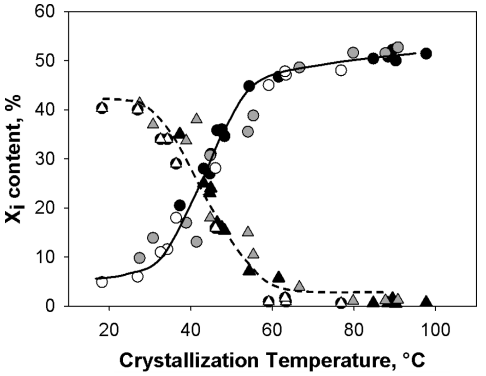

Figure 9. Phase fraction in the solidified P/E random copolymers as a function of crystallization temperature. Lines are drawn to guide the eye. Key: (●) i-PP homopolymer α-phase; (▲) i-PP homopolymer mesophase; (gray circle) random copolymer, 3.4 mol % of ethylene α-phase; (gray triangle) random copolymer with 3.4 mol % of ethylene mesophase; (○) random copolymer with 7.3 mol % of ethylene α-phase; (Δ) random copolymer with 7.3 mol % of ethylene mesophase.

dependence is shown in Figure 8. As was already deduced from the CCC diagrams, to obtain a predominant fraction of mesophase, the required cooling rate decreases with increasing counits content from around 200 °C/s for the homopolymer to below 70 °C/s for the P/E copolymer with 7.3 mol % of ethylene.

Thanks to the adopted experimental approach, the correlation between the structural features of the quenched samples and the temperature at which the ordered phases develop can be extracted. In Figure 9, the fractions of the crystalline and of the mesomorphic phases are plotted as a function of the crystallization peak temperature.

The data collected with the three samples show minor differences, if any. In fact, irrespective of the polymer composition, all data points can be considered to lie on the same sigmoidal curve, obviously with prevailing α-form in samples crystallizing at temperatures above ca. 45 °C and mesomorphic phase when structuring takes place below this temperature. The transition between the two polymorphs occurs always in a rather narrow temperature range, between 35 and 55 °C, where coexistence of the two phases in comparable amounts is revealed by WAXD.

An explanation for this peculiar behavior can be found by considering the crystallization process from the CCC perspective. We recall that the structural features eventually found in the quenched samples is determined by the time elapsed in the different CCC regions. From Figure 4, it can be appreciated that the composition dependence of the crystallization rate of the α-form is remarkably stronger than that of the mesophase. Therefore, on increasing the ethylene content in the copolymers, the large shift of the α-form CCC toward longer times is not accompanied by an analogous change in the CCC of the mesophase. Moreover, due to the rather flat shape of the upper part of the mesophase crystallization curve, a weak dependence of the crystallization temperature on the cooling rate in the region of the structural crossover is observed (see Figure 3). In line with these considerations, the temperature at which mesophase takes over the α-form is not expected to be significantly affected by the presence of ethylene counits.

At this stage, it is worth to compare our results with those previous reported in the literature on the same matter.[20,53−55] Brucato et al.[20] found no detectable difference between ZN PP homopolymer and P/E random copolymers with low amount of ethylene content (up to 3.1 mol %) in the development of the mesophase. Mileva et al.[53] studied the structure of ice−water quenched propene/ethylene metallocenic copolymers with high ethylene content, from 7 to 17 mol %, and noticed coexistence of monoclinic and mesomorphic structures under conditions in which the ZN homopolymer solidifies only in the mesomorphic form. On the contrary, only nonlamellar mesomorphic domains were detected in quenched propene/1-butene random copolymers.[53] In subsequent, more detailed, studies by the same authors,[54,55] the critical cooling rate for suppression of α-crystallization was reported to decrease on increasing the concentration of 1-butene counits.

The results of our experiments with ZN P/E random copolymers are in line with those obtained by Mileva et al. on propene/1-butene copolymers and indicate that also ethylene counits favor mesophase formation in rapidly cooled samples. All together, these experimental evidence demonstrate that the key role in favoring mesophase development is played by the presence of randomly distribute counits which hinder the formation of the α-phase. This concept can likely be generalized: any molecular feature that slows down the crystallization kinetics of the monoclinic form, i.e., constitutional as well as regio- and stereodefects, indirectly promotes the formation of the mesophase on fast cooling. Preliminary results obtained with different propene/α-olefins random copolymers and i-PPs with various stereoregularity fully support this hypothesis.[52]

Apparent deviations from this behavior[53] might likely be due to additional effects arising from the distribution of the defective units along and among the chains, an issue which deserves further investigation.

Conclusions

A new method, based on isoperibolic calorimetry, has been developed to investigate nonisothermal crystallization of polymers. Continuous cooling curve diagrams, which reveal the time and temperature coordinates at which the system crystallize, were obtained by monitoring the instantaneous sample temperature during quenching in different environments. In the case of isotactic polypropylene and its copolymers with various amounts of ethylene, the CCC curves exhibit features that are peculiar to polymorphic materials. Two different regions are easily distinguished in the temperature−time plot. The one at higher temperatures has been associated with the formation of monoclinic crystals, while the second one to the development of mesomorphic phase. This assignment has been fully validated by off-line WAXD structural characterization.

By means of the simple CCC approach, new insights on the role of counits in the development of the mesophase have been acquired. The structuring of polypropylene and its copolymers

upon fast cooling is a clear example of kinetically controlled process; notwithstanding the higher stability of the monoclinic α-form, quenched samples crystallize in the mesomorphic form. This is easily grasped from the CCC diagrams, in which it is evident that high cooling rates bypass the α-phase region leading to solidification directly in the mesophase domain.

It has been observed that constitutional defects, and probably also configurational ones, hinder the development of ordered phases to a different extent; our CCC diagrams indicate that ethylene counits remarkably decrease the crystallization kinetics of the α-form while barely affect the formation of the mesomorphic phase. Therefore, copolymers solidify in prevailing mesomorphic structure above a critical cooling rate which decreases with increasing the ethylene content, from ca. 200 °C/s for the homopolymer to less than 70 °C/s for the copolymer with 7.3 mol % of ethylene.

We believe that the simple procedure herein described can conveniently be extended to scout the effect of molecular features, as well as of any formulation of additives, in the nonisothermal crystallization of any polymer exhibiting fairly high crystallization rate.

References and Notes

(1) Rotter, G.; Ishida, H. *J. Polym. Sci., Part B: Polym. Phys.* **1992**, *30*, 625–634.
(2) Fu, Y.; Annis, B.; Boller, A.; Jin, Y.; Wunderlich, B. *J. Polym. Sci., Part B: Polym. Phys.* **1994**, *32*, 2289–2306.
(3) Piccarolo, S.; Brucato, V.; Kiflie, Z. *Polym. Eng. Sci.* **2000**, *40*, 1263–1272.
(4) McAllister, P. B.; Carter, T. J.; Hinde, R. M. *J. Polym. Sci., Polym. Phys.* **1978**, *16*, 49–57.
(5) Grebowicz, J.; Lau, J. F.; Wunderlich, B. *J. Polym. Sci., Polym. Symp.* **1984**, *71*, 19–37.
(6) Corradini, P.; Petraccone, V.; De Rosa, C.; Guerra, G. *Macromolecules* **1986**, *19*, 2699–2703.
(7) Murthy, N. S.; Minor, H.; Bednarczyk, C.; Krimm, S. *Macromolecules* **1993**, *26*, 1712–1721.
(8) Fichera, A.; Zannetti, R. *Makromol. Chem.* **1975**, *176*, 1885–1892.
(9) Marigo, A.; Marega, C.; Zannetti, R. *Macromol. Chem. Phys.* **1995**, *196*, 3577–3584.
(10) Wang, Z. G.; Hsiao, B. S.; Srinivas, S.; Brown, G. M.; Tsou, A. H.; Cheng, S. Z.D.; Stein, R. S. *Polymer* **2001**, *42*, 7561–7566.
(11) Zia, Q.; Radusch, H. J.; Androsch, R. *Polymer* **2007**, *48*, 3504–3511.
(12) Androsch, R. *Macromolecules* **2008**, *41*, 433–535.
(13) O'Kane, W. J.; Young, R. J.; Ryan, A. J.; Bras, W.; Derbyshire, G. E.; Mant, G. R. *Polymer* **1994**, *35*, 1352–1358.
(14) Martorana, A.; Piccarolo, S.; Sapoundjieva, D. *Macromol. Chem. Phys.* **1999**, *200*, 531–540.
(15) Piccarolo, S. *J. Macrom. Sci. Phys. B* **1992**, *31*, 501–511.
(16) Piccarolo, S.; Saiu, M.; Brucato, V.; Titomanlio, G. *J. Appl. Polym. Sci.* **1992**, *46*, 625–634.
(17) Sondergaard, K.; Minà, P.; Piccarolo, S. *J. Macromol. Sci.—Phys B* **1997**, *36*, 733–747.
(18) Brucato, V.; Piccarolo, S.; La Carrubba, V. *Chem. Eng. Sci.* **2002**, *57*, 4129–4143.
(19) Martorana, A.; Piccarolo, S.; Scichilone, F. *Macromol. Chem. Phys.* **1997**, *198*, 597–604.
(20) La Carrubba, V.; Piccarolo, S.; Brucato, V. *J. Appl. Polym. Sci.* **2007**, *104*, 1358–1367.
(21) Ding, Z.; Spruiell, J. E. *J. Polym. Sci., Part B: Polym. Phys.* **1996**, *34*, 2783–2804.
(22) Wagner, J.; Phillips, P. J. *Polymer* **2001**, *42*, 8999–9013.
(23) Patki, R. P.; Phillips, P. J. *Eur. Polym .J.* **2008**, *44*, 534–541.
(24) Lamberti, G.; Titomanlio, G. *Polym. Bull.* **2001**, *46*, 231–238.
(25) Brucato, V.; De Santis, F.; Giannattassio, A.; Lamberti, G.; Titomanlio, G. *Macromol. Symp.* **2002**, *185*, 181–196.
(26) Brucato, V.; De Santis, F.; Lamberti, G.; Titomanlio, G. *Polym. Bull.* **2002**, *48*, 207–212.
(27) Adamovsky, S. A.; Minakov, A. A.; Schick, C. *Thermochim. Acta* **2003**, *403*, 55–63.
(28) De Santis, F.; Adamovsky, S.; Titomanlio, G.; Schick, C. *Macromolecules* **2006**, *39*, 2562.
(29) De Santis, F.; Adamovsky, S.; Titomanlio, G.; Schick, C. *Macromolecules* **2006**, *40*, 9026.
(30) Coccorullo, I.; Pantani, R.; Titomanlio, G. *Polymer* **2003**, *44*, 307–318.
(31) Davenport, E. S.; Bain, E. C. *Trans. Soc. Min. Eng. A. I. M. E.* **1930**, *90*, 117–144.
(32) Moniz, B. J. *Metallurgy*: American Technical Publishers Inc.: Orland Park, IL, 2007
(33) Hsiung, C. M.; Cakmak, M.; White, J. L. *Polym. Eng. Sci.* **1990**, *30*, 967–980.
(34) Hsiung, C. M.; Cakmak, M. *J. Appl. Polym. Sci.* **1993**, *47*, 125–147.
(35) Spruiell, J. E.; White, J. L. *Polym. Eng. Sci.* **1975**, *15*, 660–667.
(36) Maffezzoli, A.; Kenny, J. M.; Nicolais, L. *J. Mater. Sci.* **1993**, *28*, 4994–5001.
(37) Bas, C.; Grillet, A. C.; Thimon, F.; Alberola, N. D. *Eur. Polym. J.* **1995**, *31*, 911–921.
(38) Choi, C.; White, J. L. *Polym. Eng. Sci.* **2000**, *40*, 645–655.
(39) Alamo, R. G.; Kim, M. H.; Galante, M. J.; Isasi, J. R.; Mandelkern, L. *Macromolecules* **1999**, *32*, 4050–4064.
(40) Hosier, I. L.; Alamo, R. G.; Esteso, P.; Isasi, J. R.; Mandelkern, L. *Macromolecules* **2003**, *36*, 5623–5636.
(41) Jeon, K.; Palza, H.; Quijada, R.; Alamo, R. G. *Polymer* **2009**, *50*, 832–844.
(42) De Rosa, C.; Auriemma, F.; Spera, C.; Talarico, G.; Tarallo, O. *Macromolecules* **2004**, *37*, 1441–1454.
(43) De Rosa, C.; Auriemma, F.; Ruiz de Ballesteros, O.; Resconi, L.; Camurati, I. *Macromolecules* **2007**, *40*, 6600–6616.
(44) De Rosa, C.; Auriemma, F.; Ruiz de Ballesteros, O.; Resconi, L.; Camurati, I. *Chem. Mater.* **2007**, *19*, 5122–5130.
(45) Gahleitner, M.; Jaaskelainen, P.; Ratajski, E.; Paulik, C.; Wolfschwenger, J.; Neißl, W. *J. Appl. Polym. Sci.* **2005**, *95*, 1073–1081.
(46) Forstner, R.; Peters, G. W. M.; Rendina, C.; Housmans, J. W.; Meijer, H. E. H. *J. Therm. Anal. Calorim.* **2009**, *98*, 683–691.
(47) Konishi, T.; Nishida, K.; Kanaya, T. *Macromolecules* **2006**, *39*, 8035–8040.
(48) Foresta, T.; Piccarolo, S.; Goldbeck-Wood, G. *Polymer* **2001**, *42*, 1167–1176.
(49) Lamberti, G.; De Santis, F. *Heat Mass Transf.* **2007**, *43*, 1143–150.
(50) Jeon, K.; Chiari, L.; Alamo, R. *Macromolecules* **2008**, *41*, 95–108.
(51) Alamo, R.; Vanderhart, D.; Nyden, M. R.; Mandelkern, L. *Macromolecules* **2000**, *33*, 6094–6105.
(52) Cavallo,D.; Azzurri, F.; Alfonso, G. C. To be published
(53) Mileva, D.; Androsch, R.; Radusch, H. J. *Polym. Bull.* **2008**, *61*, 643–654.
(54) Mileva, D.; Androsch, R.; Zhuravlev, E.; Schick, C. *Thermochim. Acta* **2009**, *492*, 67–72.
(55) Mileva, D.; Zia, Q.; Androsch, R.; Radusch, H. J.; Piccarolo, S. *Polymer* **2009**, *50*, 5482–5489.